A nonribosomal peptide synthetase (Pes1) confers protection against oxidative stress in *Aspergillus fumigatus*

Emer P. Reeves[1], Kathrin Reiber[1], Claire Neville[1], Olaf Scheibner[2], Kevin Kavanagh[1] and Sean Doyle[1]

1 National Institute for Cellular Biotechnology, Department of Biology, National University of Ireland Maynooth, Co. Kildare, Ireland
2 Leibniz-Institute for Natural Product Research and Infection Biology, Hans-Knoll-Institute, Jena, Germany

Aspergillus fumigatus is an important human fungal pathogen. The *Aspergillus fumigatus* genome contains 14 nonribosomal peptide synthetase genes, potentially responsible for generating metabolites that contribute to organismal virulence. Differential expression of the nonribosomal peptide synthetase gene, *pes1*, in four strains of *Aspergillus fumigatus* was observed. The pattern of *pes1* expression differed from that of a putative siderophore synthetase gene, *sidD*, and so is unlikely to be involved in iron acquisition. The Pes1 protein (expected molecular mass 698 kDa) was partially purified and identified by immunoreactivity, peptide mass fingerprinting (36% sequence coverage) and MALDI LIFT-TOF/TOF MS (four internal peptides sequenced). A *pes1* disruption mutant ($\Delta pes1$) of *Aspergillus fumigatus* strain 293.1 was generated and confirmed by Southern and western analysis, in addition to RT-PCR. The $\Delta pes1$ mutant also showed significantly reduced virulence in the *Galleria mellonella* model system ($P < 0.001$) and increased sensitivity to oxidative stress ($P = 0.002$) in culture and during neutrophil-mediated phagocytosis. In addition, the mutant exhibited altered conidial surface morphology and hydrophilicity, compared to *Aspergillus fumigatus* 293.1. It is concluded that *pes1* contributes to improved fungal tolerance against oxidative stress, mediated by the conidial phenotype, during the infection process.

The filamentous fungus *Aspergillus fumigatus* is responsible for approximately 4% of all tertiary hospital deaths in Europe [1]. *A. fumigatus* has emerged as a significant human pulmonary pathogen capable of inducing disease in patients undergoing immunosuppressive therapy or those with pre-existing pulmonary malfunction [2,3]. Invasive aspergillosis is the most serious form of the disease, involving the invasion of viable tissue and resulting in a mortality rate of 80–95% [4,5]. Circumvention of the host immune response facilitates *in vivo* fungal dissemination, and recent work has demonstrated that the modified diketopiperazine, gliotoxin, secreted by *A. fumigatus*, is capable of specifically blocking the respiratory burst in humans by inhibiting assembly of the NADPH oxidase in isolated polymorphonuclear leukocytes [6]. In addition, the release of hydroxamate-type siderophores, to facilitate iron acquisition by the organism, is also essential for fungal virulence [7].

Although classically referred to as secondary metabolites, gliotoxin and siderophores, in addition to a diverse range of other bioactive components, may

actually play a front-line role in organism growth and pathogenicity. Indeed, interest in these compounds is considerable, as many natural products are of medical or economic importance [8,9]. One mechanism that has been shown to be responsible for the biosynthesis of bioactive metabolites is nonribosomal peptide synthesis [10]. Most bioactive metabolites exhibit a peptidyl and/or polyketide composition, along with elaborate architecture including cyclic or branched-cyclic structures and modified proteogenic or nonproteogenic amino acids. Nonribosomal peptide synthetases (NRP synthetases) generally possess a colinear modular structure, with each module responsible for the activation, thiolation and condensation of one specific amino acid substrate [11]. In linear NRP synthetases, the three core domains are organized in the order condensation, adenylation and thiolation $(CAT)_n$ to form an elongation module that adds one amino acid to the growing chain. Variations on this structure include the iterative NRP synthetases characteristic of siderophore synthetases [10] or nonlinear NRP synthetases that deviate in their domain organization from the standard $(CAT)_n$ architecture. NRP synthetases that fall into this group include a peptide synthetase involved in biosynthesis of the siderophore yersiniabactin from *Yersinia* species [12] and the NRP synthetase Pes1 of *A. fumigatus* [13].

It is now clear that 14 NRPS genes are present in the genomes of *A. fumigatus* and *Aspergillus nidulans*, respectively [14,15]. Given that few functional NRP synthetase genes or proteins have been identified to date in fungi, the possibility that NRP synthetase pseudogenes may undergo transcription due to the presence of functional promoters [16,17], and the difficulties associated with predicting metabolites synthesized by cognate NRP synthetases, both gene and protein expression analysis of *pes1* was undertaken in *A. fumigatus*, coupled with the disruption of *pes1* to facilitate the assessment of the role played by *pes1* in mediating the virulence of *A. fumigatus*.

Results

Gene expression analysis

Growth curves for the three *Aspergillus* isolates, ATCC 26933, 16424 and 13073, showed that the exponential growth phase began at 12 h and extended until 48 h. Idiophase, the period when logarithmic growth had ceased, was reached at approximately 72 h, with similar biomass obtained for all three isolates (data not shown).

RT-PCR analysis was performed to investigate the relationship between fungal growth and *pes1* expres-

sion. Owing to the large size of the *pes1* transcript, different regions spanning the gene were selected for RT-PCR analysis (Fig. 1A). Primers employed were specific for adenylation domain 2 or 4 ($pes1_{A2}$, $pes1_{A4}$), the epimerase-condensation domains ($pes1_{E1-C1}$) and, for *A. fumigatus* Af293, epimerase domain 2 ($pes1_{E2}$). The presence of genomic DNA was excluded by analysis of the size difference between the genomic (617 bp) and cDNA (348 bp) amplicons of *calm* (5) (Fig. 1B).

A time-dependent difference in the expression level of *pes1* for the four *Aspergillus* isolates was evident. Amplicon presence corresponding to $pes1_{A2}$, $pes1_{A4}$ and $pes1_{E1-C1}$ confirmed that *pes1* of *A. fumigatus* ATCC 26933 was expressed at all time points (Fig. 1C–E). At the time corresponding to idiophase (72 h), the highest expression was apparent. Semiquantitative analysis of *pes1* expression was undertaken (amplicon $pes1_{A2}$; Fig. 1H) and was confirmed to be significantly increased by 38% ($P < 0.005$) over the culture period (24–72 h).

Analysis of the *pes1* expression of *A. fumigatus* ATCC 13073 (Fig. 1C–E) showed very low levels of expression at 24 h. *Pes1* expression by isolate ATCC 13073 demonstrated an increase in transcript level from 24 h to 48 h and a further significant (2.5-fold; $pes1_{A2}$) increase after 72 h ($P < 0.04$) (Fig. 1H). In contrast, upregulation of the *pes1* gene expression was not observed for *Aspergillus* isolate ATCC 16424 (Fig. 1C–E). Expression was evident at all time points during growth from 24 to 72 h; however, basal levels of expression were maintained as the culture ceased logarithmic growth, with relative expression for $pes1_{A2}$ calculated as 61%, 57% and 66% for 24, 48 and 72 h, respectively (Fig. 1H).

Simultaneous expression analysis of *A. fumigatus* *sidD* was undertaken using precisely the same culturing conditions as used for *pes1* analysis, for comparative expression analysis. The results are illustrated in Fig. 1F. Expression of *sidD* is evident at all time points (24, 48 and 72 h) and for three *Aspergillus* isolates investigated and appears to be reduced under prolonged culturing, with at least a five-fold decrease at the 72 h time point for isolates ATCC 26933 and 13073, in contrast to the observed *pes1* expression profile in both isolates.

An amplicon corresponding to $pes1_{E2}$ confirmed the presence and expression of *pes1* in the transformation recipient *pyrG* auxotrophic strain Af293.1 (Fig. 1G). In accordance with results obtained for *A. fumigatus* ATCC 26933 and 13073, *pes1* was expressed in *A. fumigatus* 293.1 at all time points, with the highest expression apparent at 72 h, thereby validating the use

of this strain in subsequent gene-disruption experiments.

In order to find whether *pes1* was expressed during fungal infection in *G. mellonella*, *A. fumigatus* ATCC 26933 conidia were injected into larvae and total RNA was isolated between $T = 24$ and 96 h. It is clear from Fig. 2 that *pes1* was expressed during fungal growth in *G. mellonella*, as the $pes1_{A2}$ cDNA was detected at 72 and 96 h postinoculation (confirmed by DNA sequence analysis; data not shown). Moreover, *pes1* expression appeared to increase relative to the actin cDNA control, which indicates elevated *pes1* expression as opposed to an increase in total fungal RNA concomitant with increased fungal mass. No $pes1_{A2}$ cDNA was detected in uninfected larval controls.
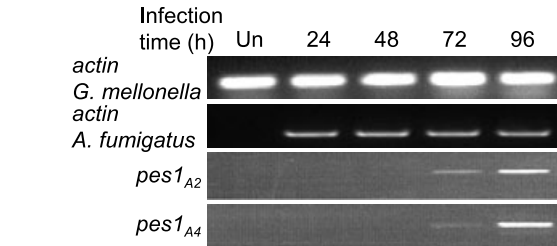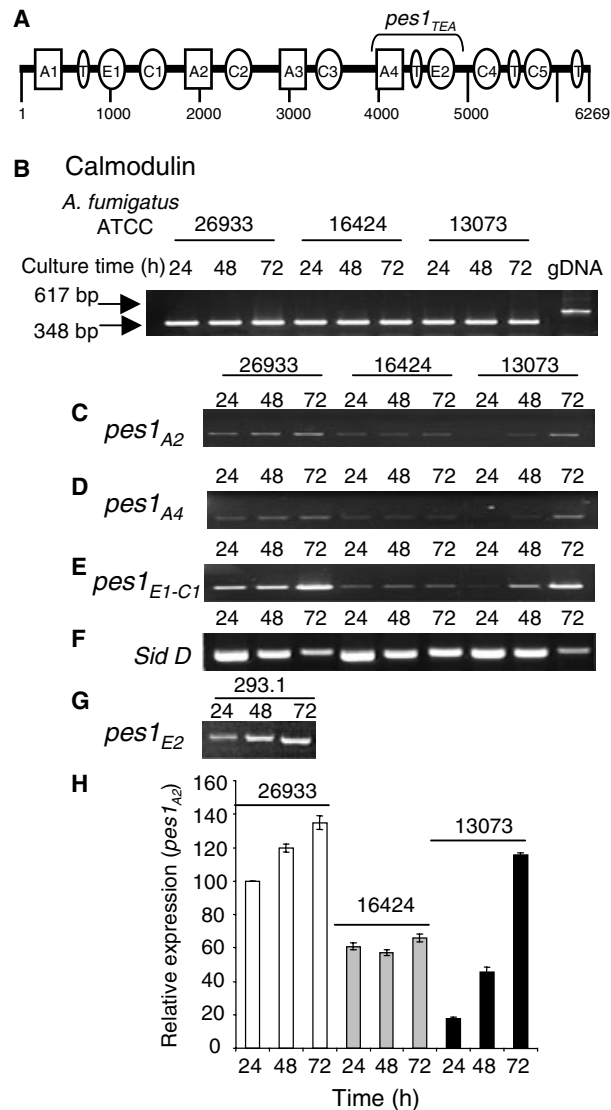

Fig. 2. Differential expression of *pes1* in infected *Galleria mellonella*. Delayed *pes1* expression was evident in *G. mellonella* infected with *Aspergillus fumigatus* ATCC 26933 conidia (1×10^5), relative to the continual presence of *A. fumigatus* actin cDNA.

Purification and immunological detection of Pes1

A recombinant protein corresponding to the second epimerase domain of *pes1* ($pes1_{E2}$) was expressed (Fig. 3A, lane 1) (34 kDa) and verified by MALDI-TOF MS; 54.5% of peptides (28% sequence coverage) obtained corresponded to the theoretical amino acid sequence of $Pes1_{E2}$ (data not shown). Polyclonal antiserum was generated, and western blot characterization of the anti-$Pes1_{E2}$ reactivity was evident (Fig. 3A, lane 2). Immunoreactivity was also evident against baculovirus-expressed recombinant $Pes1_{TEA}$ [13] (Fig. 3A, lanes 3 and 4). Immunoaffinity-purified $Pes1_{E2}$ antibodies (IgG-Pes1) were used in western blot analysis to detect recombinant $Pes1_{TEA}$, resulting in an immunoreactive band of the correct size (120 kDa), thereby

Fig. 1. Time course analysis of *pes1* gene expression. (A) Schematic diagram showing the domain architecture of *pes1* (19 190 bp nonribosomal peptide synthetase). A, AMP-binding (adenylation) domain; E, epimerase; C, condensation domain; T, thiolation domain. The epimerase 1 and condensation domain 1 (E1 and C1) occur between nucleotides 1485 and 3783. The adenylation domains 2 and 4 (A2 and A4) occur between nucleotides 4326 and 5505 and 10 710 and 11 919, respectively. Epimerase domain 2 (E2) occurs between nucleotides 9336 and 10 161, and was cloned and expressed using pProEx-Hta in *Escherichia coli*. Polyclonal antiserum was raised against this region of Pes1. The 3760 bp region ($pes1_{TEA}$) has been previously cloned and expressed [13]. (B) RT-PCR analysis of the housekeeping gene calmodulin (*calm*) confirmed the absence of DNA (gDNA, genomic DNA). (C, D, E, G) RT-PCR was used to assess *pes1* expression (by amplification of regions $pes1_{A2}$, $pes1_{A4}$, $pes1_{E1+C1}$ and $pes1_{E2}$) for *Aspergillus fumigatus* ATCC 26933, 16424, 13073 and 293.1 in cultures ranging from 24 to 72 h postinoculation. Optimal cDNA amplification was found to require 28 cycles of PCR. (F) PCR was performed on cDNA using primers to the putative siderophore synthetase-encoding gene, *sidD*. (H) Semiquantitative analysis of $pes1_{A2}$ levels. Values were normalized against the corresponding *calm* amplicon. The highest level of expression at 24 h was normalized as 100, and the results are given as relative expression (%).
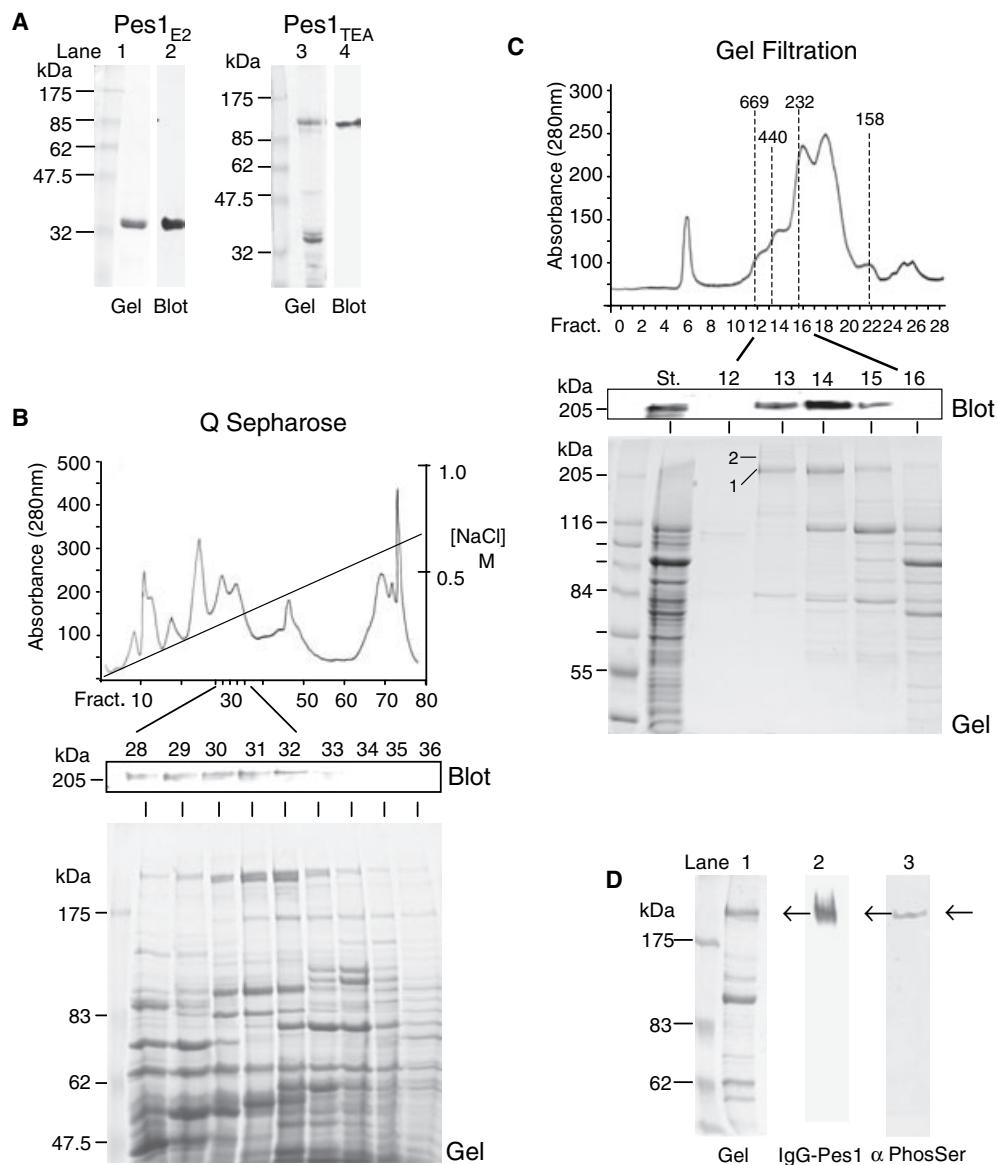
Fig. 3. Purification of the Pes1 protein from *Aspergillus fumigatus*. (A) Immunoblotting of recombinant proteins with antibodies directed to condensation domain 5 of Pes1. Lane 1, Coomassie Blue-stained SDS/PAGE gel (12.5%) of purified recombinant Pes1$_{E2}$ (34 kDa). Molecular mass markers are indicated. Lane 2, immunodetection of Pes1$_{E2}$ using Pes1$_{E2}$ antisera (1 : 2500 dilution). Lane 3, SDS/PAGE analysis of Pes1$_{TEA}$ (120 kDa). Lane 4, western analysis of Pes1$_{TEA}$ probed with affinity-purified IgG-Pes1 (1 : 1000 dilution); this confirmed that immunoaffinity-purified antiserum was functional. (B) Anion-exchange chromatography of native Pes1 from *A. fumigatus*. All fractions were subject to western analysis using IgG-Pes1, and fractions 28–32, which were found to contain the highest amounts of Pes1, were pooled. The protein profile was also visualized by Coomassie Blue-stained SDS/PAGE gels (5%). (C) Gel filtration (Superose 6) chromatography of the nonribosomal (NRP) synthetase Pes1. The protein elution profile with molecular mass markers is illustrated. The start material for the gel filtration chromatography consisted of pooled fractions from the Q-Sepharose separation step. Fractions 12–16 were found to contain immunoreactive proteins when probed with IgG-Pes1. Coomassie Blue-stained gel of the eluted fractions. Arrows indicate proteins subjected to MALDI-TOF and LIFT-TOF/TOF MS analyses. (D) SDS/PAGE and immunological analysis of the final protein preparation. Lane 1, Coomassie Blue-stained SDS/PAGE analysis illustrating the peak fraction from the Superose 6 column, which chromatographed around 500 kDa. Lane 2, western analysis of this fraction probed with IgG-Pes1. Lane 3, phosphoserine antiserum (rabbit) reactivity towards Pes1.

confirming that immunoaffinity-purified antibodies to Pes1$_{E2}$ successfully recognized this domain within the larger Pes1$_{TEA}$ protein.

Purification of native Pes1 from mycelial lysates (250 mg protein) of *A. fumigatus* ATCC 26933 was undertaken using IgG-Pes1 to detect the presence of the

protein. Pes1 was retained on a Q-Sepharose ion exchanger and eluted between 250 and 300 mM NaCl (Fig. 3B). Western blot analysis (Fig. 3B) consistently detected a single band in fractions 28–32 that migrated at 210–220 kDa. The predicted molecular mass of Pes1 is 698 kDa but no immunoreactive band within this range was visible. Analysis (5% SDS/PAGE) revealed a number of proteins of similar molecular mass (210–240 kDa) (Fig. 3C), indicative of partial proteolytic fragmentation of the NRP synthetase. Fractions containing Pes1 eluted from Q-Sepharose media (fractions 28–34; 14 mL total) were pooled, concentrated (5 mg in 500 μL) and loaded on a Superose 6 gel filtration column (Fig. 3C). Pes1 eluted from the column at an apparent molecular mass of about 500 kDa. As no protein of this approximate mass was observed by SDS/PAGE (Fig. 3C), it was possible that breakdown of the NRP synthetase occurred during SDS/PAGE sample preparation. However, it cannot be excluded the intact Pes1 did not enter the 5% SDS/PAGE gels used for these analyses. Overall, Pes1 was purified to approximately 50% purity (250 μg total protein), and a typical final protein profile is shown in Fig. 3D. A dominant protein band was obvious at approximately 220 kDa (indicated by arrow) that was associated with an immunoreactive band of the identical size using IgG–Pes1 (Fig. 3D). The observed protein was approximately 35% of the predicted mass of Pes1 and may represent the C-terminal proteolytic fragment that contained the second epimerase domain to which antibodies had been raised. Interestingly, an immunoreactive band was also detected at an identical molecular mass using phosphoserine antisera and may result from detection of the phosphoserine moiety of the 4′-phosphopantetheine cofactor bound to the NRP synthetase (Fig. 3D).

MS analysis of high molecular mass proteins

High molecular mass proteins were excised from SDS/PAGE gels and subjected to peptide mass fingerprinting by MALDI-TOF or LIFT-TOF/TOF analysis. From the MALDI-TOF spectrum of band 1 (Fig. 3C) (approximately 220 kDa), 195 out of 266 peptides were observed with identical monoisotopic values (*m/z* tolerance < 1 Da) to the theoretical digest of Pes1, thereby providing 35.9% sequence coverage of the NRP synthetase. The LIFT-TOF/TOF post-source decay fragmentation of the selected peptides with monoisotopic masses of 1262.633 and 1323.275 Da revealed the amino acid sequences QASDEGVEGTLR and NPLPDSVRVGNR, respectively. Both internal sequences were identical to the predicted sequence of Pes1. These peptides fell within the C-terminal region

of Pes1, a result consistent with the observed immunological detection of a protein of this molecular mass using affinity-purified IgG-Pes1 (Fig. 3D).

Band 2 (Fig. 3C) migrated on SDS/PAGE at a slightly higher molecular mass (approximately 240 kDa) than band 1. Sequence coverage (37.2%) of this protein was obtained (198 out of 239 peptides). MALDI LIFT-TOF/TOF fragmentation of two peptides with monoisotopic masses of 1051.65 and 1172.559 Da revealed the amino acid sequences TVARVKDLR and SIRELATRVK, respectively. As the predicted and calculated molecular mass of Pes1 is estimated to be 698 kDa (observed 440–550 kDa), it would appear that Pes1 fragmented into at least two breakdown products (Fig. 3C, protein bands 1 and 2; 220 and 240 kDa, respectively), although it is possible that further differential proteolysis had occurred.

Disruption of *pes1* in *A. fumigatus*

A Δ*pes1* mutant was generated by homologous transformation of *A. fumigatus* strain 293.1 with an 8.4 kb fragment containing the *pes1*$_{A2}$ domain (Fig. 1) disrupted by a zeocin–*pyrG*-encoding region plus 3 kb of 5′ and 3′ flanking regions, respectively (Fig. 4A). This construct was generated by double-joint PCR [18] and characterized by *Kpn*I restriction, and DNA sequence analysis confirmed the replacement of the *pes1*$_{A2}$ domain by the zeocin–*pyrG* region surrounded by intact 5′ and 3′ flanking regions of the target gene (Fig. 4B). Following protoplast transformation, PCR screening for *pes1*$_{A2}$ (negative) and zeocin (positive) colonies identified two transformants (out of 53 in total), one of which was confirmed by Southern analysis (using identical DNA loading (Fig. 4C) to lack the *pes1*$_{A2}$ domain, while containing an adjacent ABC multidrug transporter (GenBank accession number EAL90367) (Fig. 4C). Subsequent RT-PCR analysis confirmed that *pes1* expression in day 3 cultures was absent in the Δ*pes1* mutant, compared to *A. fumigatus* 293.1. ABC multidrug transporter expression was intact in both *A. fumigatus* 293.1 and the Δ*pes1* mutant (Fig. 4D). Importantly, western analysis, using immunoaffinity-purified Pes1-IgG, showed that the Pes1 protein was completely absent from the Δ*pes1* mutant. Interestingly, Pes1 was primarily located in the cytosolic fraction (C) of *A. fumigatus* 293.1 protoplast lysates, and to a lesser extent in the microsomal (M) fraction (Fig. 4E).

The *pes1* mutant displays reduced virulence

Altered growth rates have the potential to affect pathogenesis during comparison of the virulence of
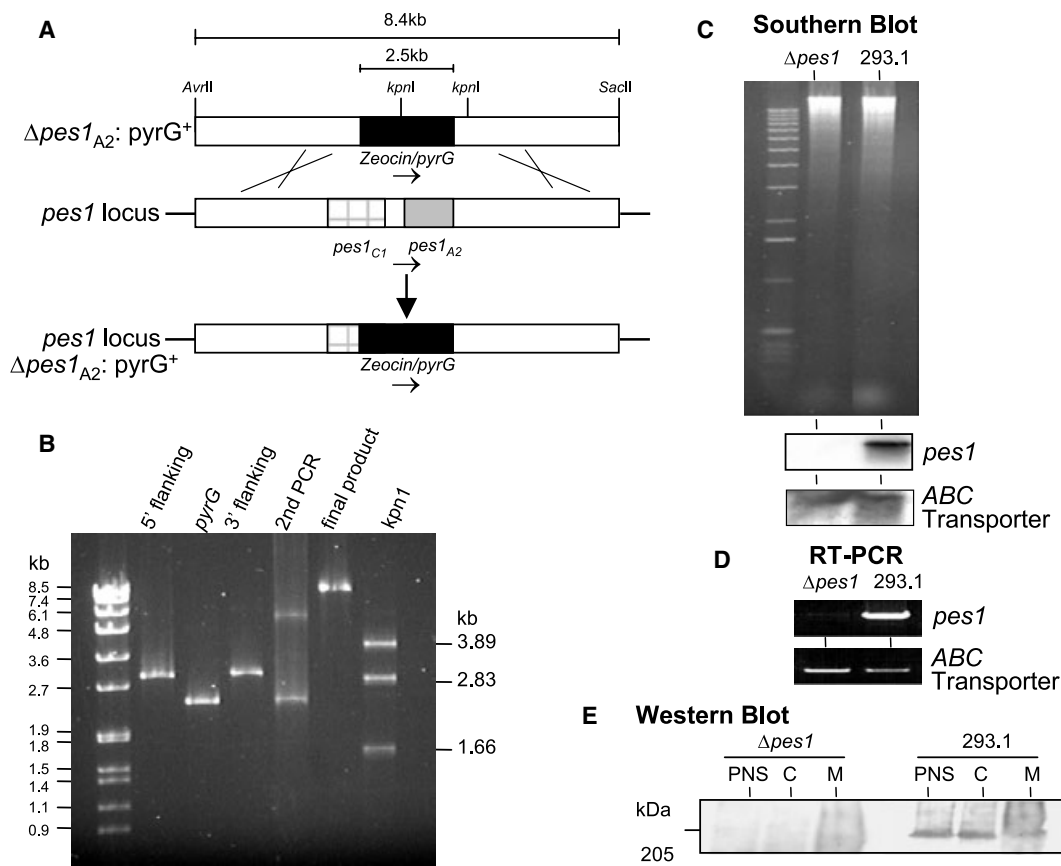
Fig. 4. Disruption of *Aspergillus fumigatus pes1*. (A) Construction of a gene deletion cassette as previously described [18]. Flanking regions (3 kb each; 5′ and 3′) encompassing the deletion target (an adenylation domain of the nonribosomal peptide (NRP) synthetase, *pes1*$_{A2}$), in addition to the pyrG–zeocin construct, were individually amplified by PCR, and then combined and subjected to nested PCR to yield a final product of 8.5 kb. (B) This product was characterized by *Kpn*I restriction and DNA sequence analysis, which confirmed the replacement of the NRP synthetase adenylation domain by the pyrG–zeocin region surrounded by intact 5′ and 3′ flanking regions of the target gene, and used for *A. fumigatus* transformation. Following transformation, mutant selection by PCR analysis of *A. fumigatus* 293.1 and putative mutants confirmed the absence of the relevant adenylation domain in the mutant strain. (C) DNA electrophoresis of restricted *A. fumigatus* 293.1 and Δ*pes1* DNA. Southern analysis confirmed the absence of *pes1* in the Δ*pes1* mutant and that a downstream ABC transporter was intact in both 293.1 and mutant strains. (D) RT-PCR analysis confirmed the absence of *pes1* expression in *A. fumigatus* Δ*pes1* relative to parental strain 293.1. Intact expression of an adjacent ABC multidrug transporter gene is evident in both strains. (E) Pes1 was not present in the postnuclear supernatant (PNS), cytosolic (C) or microsomal (M) fraction (see Experimental procedures) of the Δ*pes1* mutant, but was present in PNS and C of *A. fumigatus* 293.1.

wild-type (parental) and mutant strains, and so the growth rate of *A. fumigatus* 293.1 was compared with that of the Δ*pes1* mutant. Growth curves (Fig. 5A) showed that the exponential growth phase began at 24 h and extended until 72 h for both, and that the stationary phase was reached at 96 h, with similar biomass obtained for both 293.1 and the Δ*pes1* mutant (379 and 359 mg/100 mL culture, respectively). In order to determine whether human neutrophils killed *A. fumigatus* 293.1 and Δ*pes1* similarly, the fungicidal activity of purified human neutrophils was determined *in vitro*. The kinetics of fungal killing are shown in Fig. 5B for a ratio of neutrophils to *A. fumigatus*

conidia of 4 : 1. Killing of *A. fumigatus* 293.1 conidia occurred slowly, and only 23% of the conidia were killed after 40 min. There was a difference in the pattern of killing of conidia of *A. fumigatus* Δ*pes1*. After 40 min, 56% of the conidia were killed, and only 4% remained viable after 80 min. To further test the reduced virulence of *A. fumigatus* Δ*pes1*, we investigated the pathogenicity of the mutant using the *G. mellonella* virulence model. Figure 5C shows the mortality of larvae following infection with *Aspergillus* conidia. Avirulence of *A. fumigatus* 293.1 (*pyrG* mutant) was observed, as larvae were fully protected against infection with 1×10^6 viable conidia, as previ-
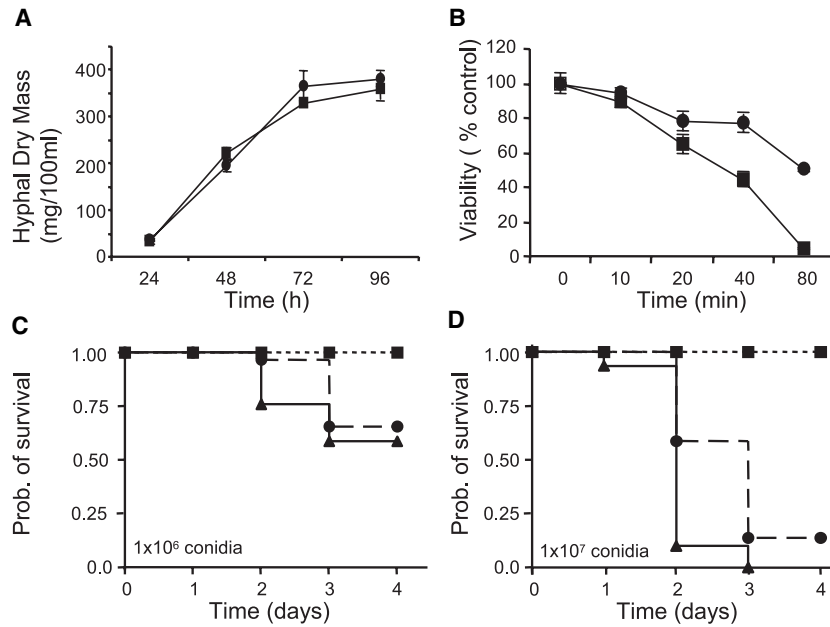
Fig. 5. Attenuated virulence of *Aspergillus fumigatus* Δ*pes1* in *in vitro* and *in vivo* virulence assays. (A) Growth curve of *Aspergillus fumigatus* 293.1 (■) and Δ*pes1* (●) in AMM supplemented with 5 mM uracil and uridine (293.1 only) and 5 mM glucose at 37 °C. (B) Fungicidal activity of human neutrophils against opsonized conidia; these were mixed at a ratio of one target organism to four immune cells in 1 mL of NaCl/P_i for the indicated periods of time, and fungal viability was determined. Reduction in survival of conidia of *A. fumigatus* 293.1 by neutrophils compared to conidia of Δ*pes1* was found to be significant ($P < 0.033$). Each value is derived from triplicate plating and the mean values (± SE) from three experiments are shown. (C, D) Survival probability plots (Kaplan–Meier) of *G. mellonella* larvae after infection with either 1×10^6 (C) or 1×10^7 (D) conidia from 293.1 (■), 293 (▲), or Δ*pes1* mutant (●) ($n = 30$). The probability of larval survival when injected with *A. fumigatus* 293 was significantly lower than with the Δ*pes1* mutant ($P < 0.045$ and $P < 0.001$ for 1×10^6 and 1×10^7 conidia, respectively).

ously described [19]. After 2 days, 25% of the larvae infected with wild-type 293 spores had died, in contrast to the attenuated virulence seen when conidia from Δ*pes1* were used ($P < 0.045$). Extending this study, larvae were infected with a higher conidial dose (1×10^7) (Fig. 5D). Conidia of the wild-type 293 strain caused the death of virtually all larvae within 2 days, while the virulence of conidia of Δ*pes1* was significantly reduced to 40%, as shown by the death of 12 of 30 larvae ($P < 0.001$). Taken together, these data establish the critical role of *pes1* in the success of *A. fumigatus* infection *in vivo*.

Effect of *pes1* disruption on conidial phenotype

Conidia of the parental *A. fumigatus* 293.1 and of the Δ*pes1* mutant were point inoculated on AMM agar plates containing 5 mM uracil and uridine (for 293.1 only) and glucose (10 mM) as the carbon source. As shown in Fig. 6A,B, disruption of *pes1* resulted in an alteration of the conidial colour phenotype. The Δ*pes1* mutant produced yellow–green conidia, as opposed to the greyish-green melanin colour of wild-type conidia. Conidia of both *A. fumigatus* 293.1 and of the Δ*pes1*

mutant were further analysed by scanning electron microscopy (Fig. 6A,B). Wild-type conidia showed a rough surface covered with ornamentation; in contrast, conidia of the Δ*pes1* mutant possessed a smoother surface with a lower degree of ornamentation on the conidial wall. In concurrence with the altered conidial phenotype, a hydrophobicity assay (Fig. 6C) of conidia from both wild-type and mutant *Aspergillus* strains revealed the Δ*pes1* mutant to be 51% more hydrophobic than the 293.1 strain ($P = 0.003$).

In order to investigate whether the altered conidial morphology affects the sensitivity to H_2O_2, conidia of the Δ*pes1* mutant or *A. fumigatus* 293.1 (as a control) were exposed to different H_2O_2 concentrations in plate diffusion assays. The inhibition zones obtained with the two different conidia were compared and are shown in Fig. 6D. Both *A. fumigatus* 293.1 and Δ*pes1* strains showed an increase in the diameter of the inhibition zone as the dose of H_2O_2 increased, but the effect was stronger in the case of the Δ*pes1* mutant (for 8 μL of 3% H_2O_2 (v/v), $P = 0.002$).

Investigation of the fungicidal effectiveness of reactive oxygen species (ROS) against the parental strain and Δ*pes1* mutant was extended to the effects of
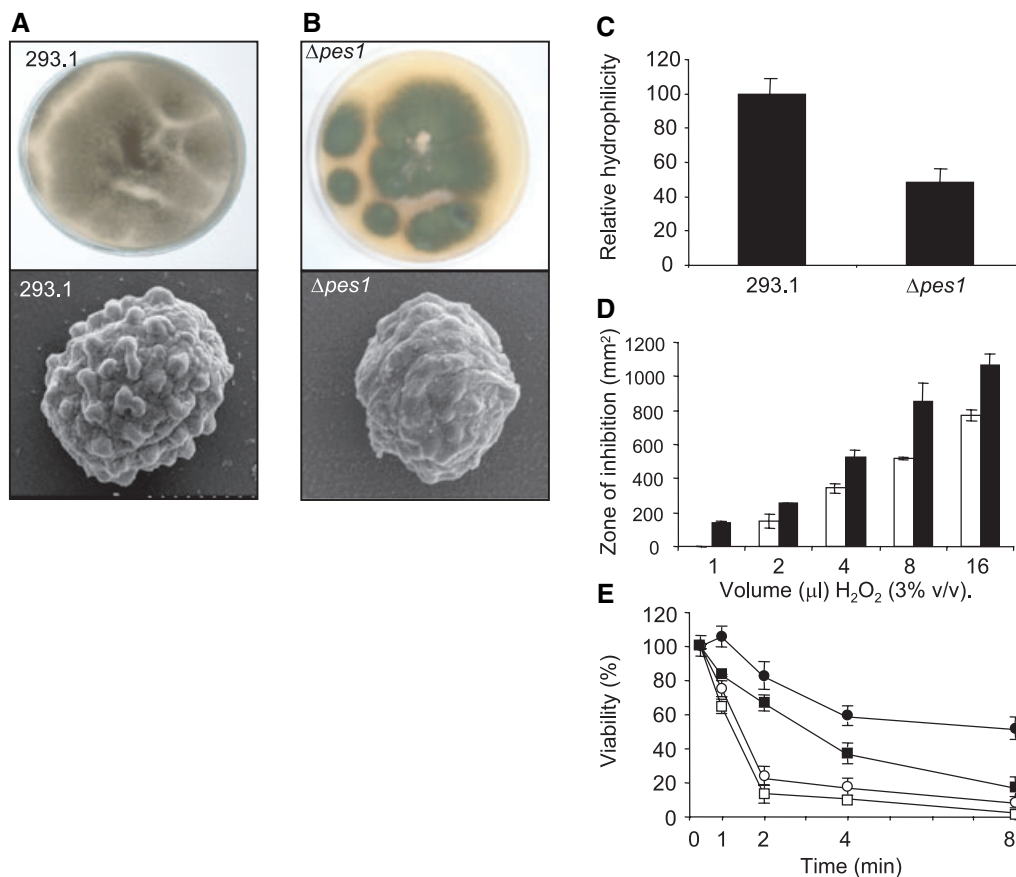
Fig. 6. Phenotypic characteristics of Δ*pes1* mutant conidia. (A and B, top panel) Spore colour of parental 293.1 (A) and Δ*pes1* mutant (B) grown on AMM plus 5 mM glucose and 2% (w/w) agar at 37 °C for 4 days. (A and B, bottom panel) Scanning electron micrographs of conidium (approximate diameter of 3 μm) of parental 293.1 (A) and of Δ*pes1* mutant (B) with strongly reduced surface ornamentation. (C) Relative hydrophilicity of conidia of parental 293.1 and Δ*pes1* mutant was determined and found to be statistically different ($P = 0.003$). Susceptibility of conidia of *Aspergillus fumigatus* 293.1 (□) and Δ*pes1* (■) strains to damage by H_2O_2 was investigated (D), and growth inhibition was plotted against the respective volume of 3% (v/v) H_2O_2. Assays were carried out in duplicate ($n = 3$) (for 8 μL of 3% H_2O_2 (v/v), $P = 0.002$). Fungicidal activity of HOCl was determined (E). The reaction mixture, NaCl/P$_i$, contained conidia of 293.1 (○,●) or Δ*pes1* (■,□)(1×10^8 mL^{-1}) and 1 (●,■) or 2.5 μM (○,□) HOCl for the indicated time points. Each line is representative of the mean (± SE) of three experiments ($P = 0.005$).

HOCl. HOCl is a strong nonradical oxidant and is the most fungicidal agent thought to be produced by neutrophils [20]. Data for incubation of *A. fumigatus* 293.1 and Δ*pes1* in 1 μM or 2.5 μM HOCl are shown in Fig. 6E. Killing by 2.5 μM HOCl occurred quickly, and over 90% of both strains were killed after just 4 min. Interestingly, there was a difference in the pattern of killing by 1 μM HOCl, and after 8 min of exposure, 51% of parental 293.1 were still viable compared to only 17% of the Δ*pes1* mutant ($P = 0.005$). These results imply that conidial morphology is closely linked to resistance against ROS and thus provide an explanation for the reduced virulence levels observed for *A. fumigatus* Δ*pes1* in *in vitro* and *in vivo* pathogenesis assays (Fig. 5).

Discussion

Here we present data that demonstrate the differential expression of a nonribosomal peptide synthetase, Pes1, in four strains of *A. fumigatus*. Native Pes1 protein was partially purified from *A. fumigatus* ATCC 26933 and found to exhibit a molecular mass of approximately 500 kDa upon gel filtration. Pes1 was identified both by immunoreactivity, using immunoaffinity-purified antibodies, and by peptide mass fingerprinting (35.9% and 37.2% sequence coverage of the N-terminal and C-terminal domains, respectively, of Pes1). Furthermore, using MALDI LIFT-TOF/TOF MS, the sequence of four peptides derived from Pes1 was determined. Deletion of *pes1* was confirmed by Southern

analysis and RT-PCR, in addition to western blot analysis, and the mutant was shown to be significantly less virulent in the *G. mellonella* model system ($P < 0.001$) and more susceptible to oxidative stress ($P = 0.002$), both in culture and during neutrophil-mediated phagocytosis. The Δ*pes1* mutant also exhibited altered conidial morphology and hydrophobicity. Taken together, these results confirm a role for *pes1* in protecting *A. fumigatus* against oxidative stress.

Semiquantitative analysis of *pes1* expression has confirmed that the gene is present, and differentially expressed, in four strains of *A. fumigatus*. Increased levels of *pes1* expression were evident in strains ATCC 26933 and 13073 over the culture time course, while expression in ATCC 16424 remained static over the 72 h culture period. Using the well-established *G. mellonella* model of fungal virulence, we have previously shown that *A. fumigatus* ATCC 26933 exhibits significantly greater virulence than either ATCC 16424 or ATCC 13073 [21], and we have hypothesized that the Pes1 product may contribute to this differential virulence (see below). Recent studies on *pes1* expression in *A. fumigatus* ATCC 26933, simultaneously determined by northern and RT-PCR analysis, showed detectable expression [13]. However, only northern analysis confirmed the constitutive nature of *pes1* expression at all time points, while RT-PCR analysis failed to detect expression at 24 h. The higher sensitivity of the RT-PCR analysis in the present work most likely accounts for this observation, and is in turn related to the low abundance level of fungal NRP synthetase transcripts – possibly only 2% of actin gene expression [22]. In the present study, we also confirmed that increased *A. fumigatus* *pes1* expression occurred in *G. mellonella* following larval inoculation. Indeed, the *G. mellonella* system has recently been used to detect upregulation of *Metarhizium anisophilae*-derived *Pr1* (which encodes a subtilisin-like protease) in infected insect larvae as the mycelia emerge and produce conidia on the surface of the cadaver [23].

It seems unlikely that *pes1* encodes a destruxin synthetase [24], as this toxin was not detected in *A. fumigatus* culture filtrates by RP-HPLC analysis (data not shown). The NRP synthetase gene of *Alternaria brassicae* has also been suggested to play a role in siderophore biosynthesis, yet upregulation of expression in a low-iron environment was not observed [16]. Direct comparison of *pes1* expression with that of *sidD* in *A. fumigatus* revealed concomitant upregulation of *pes1* and diminution of the latter, possibly implying a difference in functionality and bringing into question the classification of *pes1* as a putative siderophore

synthetase-encoding gene. Lee *et al.* [22] have recently identified a number of NRP synthetase genes in the plant pathogen *Cochliobolus heterostrophus* (NPS1-12). These authors demonstrated that only the NPS6 gene was essential for fungal virulence; however, a distinct NRP synthetase (NPS4; 20 kb)) was found to encode four adenylation, six condensation, six thiolation and three epimerase domains. Whole protein-based and adenylation domain-based phylogenetic analysis has now demonstrated that NPS4 clusters with Pes1, in particular with respect to Pes1$_{A4}$ and NPS4$_{A4}$ (supplementary Fig. S1 and Table S1). Moreover, Pes1 and NPS4 share 37% amino acid identity (56% similarity). We have also bioinformatically identified a putative *Aspergillus oryzae* NRP synthetase (GenBank accession number BAE64185.1) that exhibits significant 61% identity and 76% similarity to Pes1, and two *A. nidulans* NRP synthetases (GenBank accession numbers EAA65335 and EAA65835) that share approximately 50% identity and 67–71% similarity, respectively, with Pes1 (supplementary Fig. S1). Thus, it is now clear that the number of fungal NRP synthetases identified is set to expand as fungal genome sequence data emerge.

Microarray analysis has shown that certain disabled open reading frames are expressed in *Saccharomyces cerevisiae* [25]. Thus, the possibility that NRP synthetase pseudogenes may undergo transcription due to the presence of functional promoters, allied to the difficulty in confirming the NRP synthetase gene expression [17,22], necessitate that consideration be given to the functional identification of NRP synthetases, at the protein level, by emerging technologies. Here, monospecific, immunoaffinity-purified antibodies have been used to facilitate Pes1 purification, and MALDI LIFT-TOF/TOF MS has been deployed to unambiguously confirm the presence of native Pes1 in *A. fumigatus*. Interestingly, while the molecular mass of detectable Pes1 was shown to be about 500 kDa by gel filtration analysis, SDS/PAGE analysis demonstrated the existence of two lower molecular mass subunits. To our knowledge, immunodetection of Pes1 using phosphoserine antisera is novel; however, further studies are required to determine whether this reactivity is directed towards the phospho component of the 4′-phosphopantethine arm or against phosphoserine residues in Pes1.

Specific interruption of *pes1* gene expression and confirmation that the cognate protein product is completely absent in *A. fumigatus* is significant, as it represents one of the first successful attempts to disrupt an NRP synthetase gene in the organism. Historically, gene disruption/deletion in *A. fumigatus* has been

hampered by low frequencies of homologous recombination of the deletion construct [18]. In our hands, the double joint-PCR approach described by these authors for preparation of deletion constructs worked well and greatly simplified construct generation. Furthermore, although not used during the present study, the demonstration that *A. fumigatus* Δ*akuA* [26] and Δ*akuB* [27] mutants can yield up to 80–95% site-specific homologous transformation, following protoplast transformation, is significant, as it should greatly improve the success rate for gene deletion in this organism.

G. mellonella is attracting ever-increasing attention as a model organism for the study of microbial virulence in general [23], and *Aspergillus* virulence in particular [26,28]. The *in vitro* generation of ROS has been observed in the self-defence system of *G. mellonella*, with both O_2^- [29] and its dismutation product H_2O_2 [30] being found in phagocytic cells. The significantly reduced virulence of the Δ*pes1* mutant, compared to *A. fumigatus* Af293, is evident at conidial loads of both 10^6 and 10^7 per larvae. These data confirm the suitability of the *G. mellonella* virulence model to detect alterations in the pathogenicity of *A. fumigatus* mutants and complement the recent demonstration that the system can also be used to confirm lack of virulence following gene deletion [26]. Thus, the elucidation of significantly reduced virulence of the *A. fumigatus* Δ*pes1* mutant further enhances the utility of this model system, which provides an alternative, or complementary, approach to the use of animal model systems.

ROS production following activation of the respiratory burst NADPH oxidase of neutrophils is required for optimal antimicrobial function, and its importance is demonstrated by the syndrome of chronic granulomatous disease (CGD) [31]. CGD is a rare condition and is associated with the absence of the generation of ROS. ROS have widely been thought to be responsible for the killing of phagocytosed microorganisms, either directly (O_2^- and H_2O_2) or by acting as substrate for myeloperoxidase-mediated halogenation (HOCl) [20]. In previous studies, inhibitors of the NADPH oxidase that decreased the production of ROS inhibited the killing of *A. fumigatus* [32], and invasive aspergillosis is the primary cause of death in patients suffering from CGD [33]. The primary observations of this study on neutrophil-mediated killing of *A. fumigatus* 293.1 conidia highlight the importance of *pes1* as an important contributor to fungal virulence. Killing of conidia demonstrated a clear time-dependent index, with neutrophils exhibiting the ability to kill conidia of *A. fumigatus* Δ*pes1* at a higher rate than those of 293.1. The fungicidal effects of increasing concentra-

tions of H_2O_2 and HOCl were studied, with greater sensitivity to both ROS being exhibited by *A. fumigatus* Δ*pes1*. Oxidants such as HOCl are known to react with thiol groups, thioesters, and aliphatic or aromatic groups [34]. Most of these reactions lead to a loss in oxidative capacity, resulting in the loss of microbial properties. However, the effect of HOCl is directly related to the presence of protein on the surface or in the surrounding environment [35], and higher amounts of protein will consume the available HOCl. The Δ*pes1* mutant displayed differences in conidial surface morphology and was shown to be significantly more hydrophobic than the parental 293.1 strain. Previous studies have implicated both pigment and altered conidial protein surface in increased susceptibility to oxidative damage [36,37]; accordingly, the differences in conidial ornamentation observed for *A. fumigatus* Δ*pes1* may render this mutant more sensitive to applied ROS. Interestingly, upregulation of *pes1* expression was not observed following H_2O_2-induced oxidative stress in cultures of *A. fumigatus* 293.1 grown in either Sabouraud or 5% FBS in MEM (data not shown). Moreover, expression of neither of the two *A. nidulans* orthologues of *pes1* (GenBank accession numbers EAA65335 and EAA65835; supplementary Fig. S1 and Table S1) was upregulated following exposure to H_2O_2 [38].

Sheppard *et al.* [39] have recently described the importance of the transcription factor StuA in the acquisition of developmental competence in *A. fumigatus*. These authors showed *pes1* expression to be the most significantly altered (downregulated) in an *A. fumigatus stuA* mutant, following whole genome microarray analysis, during the onset of developmental competence. Significantly, the *stuA* mutant exhibited enhanced sensitivity to H_2O_2-induced oxidative stress, and a small, although not significant, reduction in virulence in a murine model system. This pattern of altered resistance to oxidative stress is similar to that observed in the Δ*pes1* mutant, so it is possible that the Pes1 peptide product may be involved in mediating the downstream effects of StuA-induced gene expression. Secondary metabolites may play a significant role in fungal development [14]. For example, in *Aspergillus parasiticus* and *A. nidulans*, chemical inhibition of polyamine biosynthesis inhibits sporulation, in addition to aflatoxin and sterigmatocystin production, respectively [40]. As late growth phase expression of *pes1* is evident, it is possible that the Pes1 peptide product may be involved in the sporulation process of this fungus.

In summary, our data show that *pes1* expression is temporally regulated in *A. fumigatus* both *in vitro*

Table 1. Nucleotide sequence of oligonucleotide primers used to amplify *Aspergillus fumigatus* genes from *A. fumigatus* genomic DNA and cDNA.

Primers	Sequence (5′- to 3′)
pes1$_{A2}$ forward	GGCTCTGGAACTGAATAAAGCGAC
pes1$_{A2}$ reverse	GTCCCATATATCCGCTTGCAATCT
pes1$_{A4}$ forward	TCTGACTCCGTCGATAGCTAGCAT
pes1$_{A4}$ reverse	CCAGATCCTCACGACTGATAAGCTC
pes1$_{C2}$ forward	GAGATCTAGATACCCATGCAGCCCTGTC
pes1$_{C2}$ reverse	GAGAAAGCTTGTCAACTTGAATGCGGGTAGG
pes1$_{E1-C1}$ forward	CGCTGGCGAACACATTATATGA
pes1$_{E1-C1}$ reverse	ACGAATTACTTGCAGCCGCTT
sidD forward	ACGCAACCGACTGGTTGTT
sidD reverse	ATTCGTGCGAGACTCGGAT
Calmodulin forward	CCGAGTACAAGGAAGCTTTCTC
Calmodulin reverse	GAATCATCTCGTCGACTTCGTCGTCAGT
Aspergillus fumigatus actin forward	CGAGACCTTCAACGCTCCCGCCTTCTACGT
Aspergillus fumigatus actin reverse	GATGACCTGACCATCGGGAAGTTCATAGGA
5′ flanking forward	CTAGCTGGTGAAGCAATGTCTCCGCAACATTTGGCGACATGGTCTCATAT
5′ flanking reverse	GGCCGAGGAGCAGGACTGAGAATTCTTTGCGGTCTTCCTGAAGCTGACCACTGT
3′ flanking forward	CATTGTTTGAGGCGAATTCGATATCGAGGCTCAGAACCTCCCTGCGCAGACGCG
3′ flanking reverse	GGCCTCCCTAAGCTTCTGGACCTTTTCGCGTGTTGCTTCCGACATAGGAACGAG
zeocin–pyrG forward	GAATTCTCAGTCCTGCTCCTCGGCC
zeocin–pyrG reverse	GATATCGAATTCGCCTCAAACAATG
Nested forward	GAGACCTAGGAAGCAATGTCTCCGCAACATTTGGCGACATGGTCTCATAT
Nested reverse	GAGACCGCGGAAGCTTCTGGACCTTTTCGCGTGTTGCTTCCGACATAGGA

and during infection of *G. mellonella*, respectively. Pes1 protein was also demonstrated in *A. fumigatus*, thereby confirming that *pes1* is a functional gene. Disruption of *pes1* led to decreased fungal virulence, and increased susceptibility to oxidative stress and neutrophil-mediated killing, in addition to altered conidial morphology and hydrophobicity. Taken together, these data strongly suggest that *pes1* significantly contributes to the resistance of *A. fumigatus* to oxidative stress.

Experimental procedures

Chemicals

All chemicals and reagents were purchased from Sigma-Aldrich (Sigma-Aldrich Chemical Co., Poole, UK), unless stated otherwise.

Microorganisms and culture conditions

Clinical isolates of *A. fumigatus* used in this study included ATCC 26933, ATCC 16424 and ATCC 13073 (obtained from the American Type Culture Collection, MD, USA) with culture conditions and growth curves constructed as previously described [21]. The *A. fumigatus* strain Af293 and the transformation recipient *pyrG* auxotrophic strain Af293.1 were obtained from the Fungal Genetics Stock Center, Kansas City, USA [41] and cultured on *Aspergillus* minimal medium (AMM), supplemented with 5 mM uridine and uracil (auxotrophic strain) and 1% (w/v) glucose. *Aspergillus* growth curves were obtained as previously described [21].

Isolation of genomic DNA, RNA and RT-PCR amplification

Preliminary sequence data were obtained from The Institute for Genomic Research website at http://www.tigr.org. The extraction of genomic DNA was as previously described [42]. Fungal RNA was isolated and purified from crushed hyphae of *Aspergillus*, employing the Rneasy™ plant mini kit (Qiagen, Crawley, UK). Total RNA was extracted from *Aspergillus*-infected *G. mellonella* using TRI REAGENT™ according to the manufacturer's instructions. Prior to cDNA synthesis, RNA was treated with DNase I. cDNA synthesis from mRNA (1 µg) was performed using the SuperScript™ kit (Invitrogen, Paisley, UK) using oligo(dT) primers. PCR was performed using AccuTaq polymerase with 1–10 ng genomic DNA as template. PCR was performed using the primers summarized in Table 1. PCR conditions were as follows: 95 °C denaturing for 5 min (95 °C denaturing for 30 s, 55 °C annealing for 30 s, 72 °C extension for 6 min) × 28 cycles; and 72 °C extension for 6 min. The gene encoding calmodulin (*calm*), which is constitutively expressed in *Aspergillus*

fumigatus, served as a control in RT-PCR experiments [43]. Primers for *actin* of *G. mellonella* were as previously described [23]. Visualization of amplicons was performed using an 'Eagle-Eye II' digital still video system (Stratagene, La Jolla, CA, USA). Densitometric quantification of PCR products was performed using GENETOOLS software (Syngene, Cambridge, UK).

Cloning and expression of *pes1*$_{E2}$

The *pes1*$_{E2}$ sequence was amplified from *A. fumigatus* ATCC 26933 genomic DNA, using primers incorporating terminal *Hin*dIII and *Xba*I sites (New England Biolabs, Ipswich, UK). PCR products were cloned directly into the pProEx-Hta^{TM} expression vector (Invitrogen), and the resultant expression vector containing *pes1*$_{E2}$ was transformed into *Escherichia coli* strain DH5α. After confirmatory DNA sequence analysis, expression of *pes1*$_{E2}$ was induced and recombinant Pes1$_{E2}$ purified [44]. Recombinant Pes1$_{TEA}$ (Fig. 1) was purified as previously described [13].

Antiserum production

Rabbit antiserum was raised against purified Pes1$_{E2}$ using standard protocols [44]. Pes1-specific antibodies were immunoaffinity purified against Pes1$_{E2}$ immobilized on nitrocellulose, eluted with 0.1 M glycine/HCl, pH 2.9, and immediately neutralized with 0.5 M NaOH. Immunoaffinity-purified antibodies (termed IgG-Pes1) were used (1 : 1000) for 1 h in western blot analyses. Phosphoserine antisera (Abcam, Cambridge, UK) was used at a dilution of 1 : 250 and incubated for 16 h at 4 °C. Horseradish peroxidase-conjugated donkey anti-rabbit IgG (1 : 5000 dilution) (Amersham Biosciences, Freiburg, Germany) was used to detect reactive bands by the enhanced chemiluminescence (ECL) system (Pierce Biotechnology, Cramlington, UK).

Protein purification

Hyphae were harvested from 4 L of cultured *A. fumigatus* ATCC 26933. All protein isolation and purification steps were performed at 4 °C. Protein concentrations were determined using the Bradford method with BSA as a standard. Hyphae were washed twice in NaCl/P$_i$ and ground to a fine powder under liquid N$_2$. The ground hyphae were resuspended in Break Buffer [45], in the presence of protease inhibitors [46], and sonicated (Bandelin Sonopuls, Progen Scientific Ltd., Mexborough, UK) for 3×5 s at maximum power. After centrifugation for 10 min at 40 000 *g* using a Sorvall Instruments RC5C centrifuge (GSA rotor) (Thermo Electron Corp., Asheville, NC, USA), the supernatant (approximately 250 mg of protein) was chromatographed successively as follows. Starting material was loaded onto

Q-Sepharose (1.5×8 cm, 1 mL·min^{-1}, 2 mL fractions collected, eluted with a 100 mL linear gradient of 0–1 M NaCl in Break Buffer). Peak fractions containing native Pes1 were identified by immunoreactivity (IgG-Pes1), pooled (14 mL) and concentrated to 0.5 mL using a Centricon 30 (Millipore, Cork, Ireland). The concentrated material (approximately 850 μg of total protein) was further purified by gel filtration using an ÄKTA Purifier 100 system (Amersham Biosciences), whereby a Superose 6 column (10×300 mm) was equilibrated in Break Buffer supplemented with 500 mM NaCl at a flow rate of 0.4 mL·min^{-1}. The concentrated material from Q-Sepharose was loaded on the column and 0.5 mL fractions were collected. As molecular mass markers, thyroglobulin (669 kDa), ferritin (440 kDa), catalase (232 kDa) and aldolase (158 kDa) were used separately. Protease inhibitors were included in all buffers used for chromatography [46]. Electrophoretic analysis was carried out using 5% SDS/PAGE to facilitate detection of high molecular mass proteins.

MS

Peptide mass fingerprinting and LIFT-TOF/TOF MS analysis of trypsin-digested Pes1 were carried out using a Bruker ultraflex LIFT-TOF/TOF (Bruker, Rheinstetten, Germany), as previously described [46]. Only peptides with high signal intensity were subject to LIFT-TOF/TOF analysis [47] and resultant spectra processed using FLEXANALYSIS software (Bruker). Database searches and sequence comparisons were carried out via MASCOT inhouse server (Matrix Science, London, UK) and BIOTOOLS (Bruker), respectively.

Disruption of *A. fumigatus pes1*

Disruption of *pes1* was performed using the double-joint PCR method as previously described [18]. The first-round PCR generated amplicons containing 5′ and 3′ flanking regions of *pes1*$_{A2}$ and carried 25 bp of homologous sequence overlapping with the ends of the *pyrG* selection marker. The sequences of primers used to amplify the flanking regions (5′ and 3′ flanking forward and reverse) are given in Table 1. The *pyrG* selection marker was amplified from the pCDA21 plasmid (a gift from AA Brakhage, Leibnitz-Institute for Natural Product Research and Infection Biology) using primers *pyrG* forward and *pyrG* reverse (Table 1). Conditions for the first-round PCR were as follows: 93 °C for 5 min; four cycles of 93 °C for 30 s, 58 °C for 2 min and 72 °C for 3 min; 24 cycles of 93 °C for 30 s, 60 °C for 2 min and 72 °C for 3 min; and finally 72 °C for 10 min. PCR products were gel purified (gel extraction kit, Qiagen), and for the second-round PCR, 1 μL of both the 5′ flanking and 3′ flanking amplicons were mixed with 3 μL of the purified *pyrG* amplicon. The second-round PCR

conditions (using Long Expand polymerase; Roche Diagnostics GmbH, Mannheim, Germany) were: 94 °C for 2 min; 15 cycles of 94 °C for 45 s, 62 °C for 2 min, 68 °C for 12 min; and finally 15 min postpolymerization. Nested primers for the third-round PCR were designed (Table 1) including a 5′-*Avr*II (New England Biolabs) restriction site on the forward primer and a 3′-*Sac*II (New England Biolabs) restriction site on the reverse primer. Conditions for the third-round PCR were as previously described [18]. Prior to cloning into the pCR 2.1-TOPO expression vector, PCR products were confirmed on the basis of size, sequencing (Lark Technologies, Takeley, UK) and *Kpn*I (New England Biolabs) restriction enzyme digestion.

Aspergillus transformation

A. fumigatus protoplasts were prepared from conidia of *A. fumigatus* 293.1 grown for 7 h at 37 °C in AMM supplemented with 5 mM uracil and uridine. Hyphal cells were harvested by centrifugation at 200 g for 15 min (IEC Centra CL3R, swingout rotor, Biosciences, Dublin, Ireland) and resuspended in 40 mL of Protoplasting Buffer (0.4 M (NH_4)$_2$SO$_4$, 50 mM potassium citrate, 10 mM MgSO$_4$, 0.5% (w/v) sucrose, pH 6.2) containing Zymolase (120 mg), Driselase (400 mg), Glucanase (200 mg), BSA (400 mg) and 10 mM 2-mercaptoethanol. The suspension was incubated at 37 °C for 1.5–2 h, and filtered through Miracloth (Calbiochem, Bad Soden, Germany), and protoplasts were pelleted by gentle centrifugation (200 g, 5 min). Protoplasts (1×10^7) were resuspended in 200 μL of Transformation Buffer (TM) (0.6 M KCl, 50 mM CaCl$_2$, 10 mM methanesulfonic acid, pH 6.0) containing 10–20 μg of transformation DNA, and 100 μL of polyethylene glycol (PEG) solution (25% (w/v) PEG 6000, 50 mM CaCl$_2$, 0.6 M KCl, 10 mM Tris/HCl, pH 7.5). The suspension was chilled to 4 °C for 15 min, and a further 1 mL of PEG solution added at room temperature for 15 min. TM (10 mL) was added to the mixture, and the transformed protoplasts were pelleted by centrifugation (200 g, 5 min). Protoplasts were resuspended in 500 μL of TM, and 50 μL aliquots were mixed with 10 mL of AMM (minus uracil and uridine) containing 1 M sorbitol as osmotic stabilizer plus 2% (w/v) molten agar, and then poured onto minimal medium agar plates. Putative transformants became visible after 2 days of incubation at 37 °C and were subcultured onto AMM. Southern blot analysis was carried out as previously described [48].

Subcellular fractionation and localization of Pes1

To localize Pes1, protoplasts were prepared as described above and homogenized in Break Buffer containing 10% (v/v) glycerol. A postnuclear supernatant (PNS) was centrifuged (40 000 g for 3 h at 4 °C in a Beckman SW40 TI) to yield microsomal (M) pellet and soluble cytosol (C) fractions

as previously described [49]. Fractions were analysed by SDS/PAGE and immunodetection using immunoaffinity-purified antibodies, IgG-Pes1.

In vitro killing of conidia by human neutrophils

Neutrophils were purified from fresh human blood by dextran sedimentation and centrifugation through Ficoll/Hypaque as previously described [50]. Cells (5×10^8) were incubated at 37 °C in 1 mL NaCl/P$_i$ in a rapidly stirred chamber. IgG opsonized conidia were added (1.25×10^8) and killing measured as described by Segal *et al.* [51], omitting lysostaphin. Results were calculated as the mean ($\pm$ SE) from three experiments with colony counts performed in triplicate for each sample and expressed as a percentage of the original numbers at time zero.

In vivo testing of virulence

A. fumigatus strains were grown on AMM for 14 days at 37 °C. Conidia were harvested [21] and infection studies carried out in the insect model *G. mellonella*, according to standard protocols [29,52]. A group of 30 larvae were infected with the *A. fumigatus* 293.1, 293 or Δ*pes1* by injecting 20 μL of an inoculum suspension (per larvae) containing 1×10^6 or 1×10^7 conidia into the hemocoel/body cavity via the last proleg. Larvae were observed for mortality, twice daily, over a period of 7 days.

Scanning electron microscopy (SEM)

Conidia were fixed in 5% (v/v) formaldehyde and 2% (v/v) glutaraldehyde in cacodylate buffer (0.1 M cacodylate, 0.01 M CaCl$_2$, 0.01 M MgCl$_2$, 0.09 M sucrose, pH 6.9) and washed with cacodylate buffer and then with TE buffer (10 mM Tris/HCl, 2 mM EDTA, pH 6.9). Conidia were placed onto poly(L-lysine) coated glass slides and SEM carried out as previously described [28].

In vitro test for H_2O_2 and HOCl sensitivity

Conidia of *A. fumigatus* 293.1 and Δ*pes1* were harvested from AMM plates [21] and resuspended in NaCl/P$_i$ at a final concentration of 1×10^8 conidia/mL. AMM agar (100 mL) with added uracil and uridine (293.1 only) was cooled to 38 °C and 1 mL of conidia added before pouring into a Petri dish (240×240 mm). Nine holes with a diameter of 1 cm were punched into each agar plate and different amounts of 3% (v/v) H_2O_2 solution applied. Plates were incubated for 16 h at 37 °C and inhibition zones determined as an average of three specimens each.

Conidia (1×10^8/mL) were suspended in 1 mL of NaCl/P$_i$ and exposed to two different concentrations of HOCl (1 and 2.5 μM) at 37 °C. After mixing for 1, 2, 4 and

8 min, aliquots were removed and diluted 1 : 10 in ice-cold AMM. Serial 10-fold dilutions were then made, and plated in triplicate for each specimen; results were calculated as the mean ($\pm$ SE) from three separate experiments. The pH remained stable during assays to within 0.15 pH units of the starting pH.

Hydrophobicity assay

Conidia were harvested [21], washed twice and suspended in 0.05 M sodium phosphate buffer (pH 7.4) containing 0.15 M NaCl to $D_{540\ nm} = 0.4$. The conidial suspension was treated with xylene (2.5 : 1, v/v), vigorously mixed for 2 min, and allowed to settle for 20 min. The absorbance of the aqueous phase was then determined at 540 nm and the relative hydrophilicity determined [53].

Acknowledgements

References

1 Denning DW, Anderson MJ, Turner G, Latge JP & Bennett JW (2002) Sequencing the *Aspergillus fumigatus* genome. *Lancet Infect Dis* **2**, 251–253.

2 Daly P & Kavanagh K (2001) Pulmonary aspergillosis: clinical presentation, diagnosis and therapy. *Br J Biomed Sci* **58**, 197–205.

3 Kontoyiannis DP & Bodey GP (2002) Invasive aspergillosis in 2002: an update. *Eur J Clin Microbiol Infect Dis* **21**, 161–172.

4 Denning DW (1996) Therapeutic outcome in invasive aspergillosis. *Clin Infect Dis* **23**, 608–615.

5 Denning DW (1998) Invasive aspergillosis. *Clin Infect Dis* **26**, 781–805.

6 Tsunawaki S, Yoshida LS, Nishida S, Kobayashi T & Shimoyama T (2004) Fungal metabolite gliotoxin inhibits assembly of the human respiratory burst NADPH oxidase. *Infect Immun* **72**, 3373–3382.

7 Schrettl M, Bignell E, Kragl C, Joechl C, Rogers T, Arst Jr HN, Haynes K & Haas H (2004) Siderophore biosynthesis but not reductive iron assimilation is essential for *Aspergillus fumigatus* virulence. *J Exp Med* **200**, 1213–1219.

8 Bennett JW & Klick M (2003) Mycotoxins. *Clin Microbiol Rev* **16**, 497–516.

9 Jarvis BB & Miller JD (2005) Mycotoxins are harmful indoor air contaminants. *Appl Microbiol Biotechnol* **66**, 367–372.

10 Mootz HD, Schwarzer D & Marahiel MA (2002) Ways of assembling complex natural products on modular nonribosomal peptide synthetases. *Chembiochem* **3**, 490–504.

11 Kleinkauf H & von Dohren H (1990) Nonribosomal biosynthesis of peptide antibiotics. *Eur J Biochem* **192**, 1–5.

12 Gehring AM, DeMoll E, Fetherston JD, Mori I, Mayhew GF, Blattner FR, Walsh CT & Perry RD (1998) Iron acquisition in plague: modular logic in enzymic biogenesis of yersiniabactin by *Yersinia pestis*. *Chem Biol* **5**, 573–586.

13 Neville C, Murphy A, Kavanagh K & Doyle S (2005) A 4′-phosphopantetheinyl transferase mediates non-ribosomal peptide synthetase activation in *Aspergillus fumigatus*. *Chembiochem* **6**, 679–685.

14 Keller NPG, Turner G & Bennet JW (2005) Fungal secondary metabolism − from biochemistry to genomics. *Nat Rev Microbiol* **3**, 937–947.

15 Nierman WC, Pain A, Anderson MJ, Wortman JR, Kim HS, Arroyo J, Berriman M, Abe K, Archer DB, Bermejo C, *et al.* (2005) Genomic sequence of the pathogenic and allergenic filamentous fungus *Aspergillus fumigatus*. *Nature* **438**, 1151–1156.

16 Guillemette T, Sellam A & Simoneau P (2004) Analysis of a nonribosomal peptide synthetase gene from *Alternaria brassiciae* and flanking genomic sequences. *Curr Genet* **45**, 214–224.

17 Vizcaino JA, Sanz L, Cardoza RE, Monte E & Gutierrez S (2005) Detection of putative peptide synthetase genes in *Trichoderma* species: application of this method to the cloning of a gene from *T. harzianum* CECT 2413. *FEMS Microbiol Lett* **244**, 139–148.

18 Yu JH, Hamari Z, Han H, Seo JA, Reyes-Dominguez Y & Scazzocchio C (2004) Double-joint PCR: a PCR-based molecular tool for gene manipulations in filamentous fungi. *Fungal Genet Biol* **41**, 973–981.

19 D'Enfert C, Diaquin M, Delit A, Wuscher N, Debeaupuis JP, Huerre M & Latge JP (1996) Attenuated virulence of uridine-uracil auxotrophs of *Aspergillus fumigatus*. *Infect Immun* **64**, 4401–4405.

20 Klebanoff SJ (1975) Antimicrobial mechanisms in neutrophilic polymorphonuclear leukocytes. *Semin Hematol* **12**, 117–142.

21 Reeves EP, Messina CG, Doyle S & Kavanagh K (2004) Correlation between gliotoxin production and virulence of *Aspergillus fumigatus* in *Galleria mellonella*. *Mycopathologia* **158**, 73–79.

22 Lee BN, Kroken S, Chou DY, Robbertse B, Yoder OC & Turgeon BG (2005) Functional analysis of all nonribosomal peptide synthetases in *Cochliobolus heterostrophus* reveals a factor, NPS6, involved in virulence and resistance to oxidative stress. *Eukaryot Cell* **4**, 545–555.

23 Small CL & Bidochka MJ (2005) Up-regulation of Pr1, a subtilisin-like protease, during conidiation in the insect pathogen *Metarhizium anisopliae*. *Mycol Res* **109**, 307–313.

24 Soledade M, Pedras MSC, Zaharia LL & Ward DE (2002) The destruxins: synthesis, biosynthesis, biotransformation, and biological activity. *Phytochemistry* **59**, 579–596.

25 Harrison P, Kumar A, Lan N, Echols N, Synder M & Gerstein M (2002) A small reservoir of disabled ORFs in the yeast genome and its implications for the dynamics of proteome evolution. *J Mol Biol* **316**, 409–419.

26 Krappmann S, Sasse C & Braus GH (2006) Gene targeting in *Aspergillus fumigatus* by homologous recombination is facilitated in a nonhomologous end-joining-deficient genetic background. *Eukaryot Cell* **5**, 212–215.

27 da Silva Ferreira ME, Kress MR, Savoldi M, Goldman MH, Hartl A, Heinekamp T, Brakhage AA & Goldman GH (2006) The akuB (KU80) mutant deficient for non-homologous end joining is a powerful tool for analyzing pathogenicity in *Aspergillus fumigatus*. *Eukaryot Cell* **5**, 207–211.

28 Maeker C, Rohde M, Brakhage AA & Brock M (2005) Methylcitrate synthase from *Aspergillus fumigatus*. Propionyl-CoA affects polyketide synthesis, growth and morphology of conidia. *FEBS J* **272**, 3615–3630.

29 Bergin D, Reeves EP, Renwick J, Wientjes FB & Kavanagh K (2005) Superoxide production in *Galleria mellonella*: identification of proteins homologous to the NADPH oxidase complex of human neutrophils. *Infect Immun* **73**, 4161–4170.

30 Slepneva IA, Glupov VV, Sergeeva SV & Khramtsov VV (1999) EPR detection of reactive oxygen species in hemolymph of *Galleria mellonella* and *Dendrolimus superans sibiricus* (Lepidoptera) larvae. *Biochem Biophys Res Commun* **264**, 212–215.

31 Goldblatt D & Thrasher AJ (2000) Chronic granulomatous disease. *Clin Exp Immunol* **122**, 1–9.

32 Philippe B, Ibrahim-Granet O, Prevost MC, Gougerot-Pocidalo MA, Sanchez Perez M, Van der Meeren A & Latge JP (2003) Killing of *Aspergillus fumigatus* by alveolar macrophages is mediated by reactive oxidant intermediates. *Infect Immun* **71**, 3034–3042.

33 Winkelstein JA, Marino MC, Johnston RB Jr, Boyle J, Curnutte J, Gallin JI, Malech HL, Holland SM, Ochs H, Quie P, Buckley RH, Foster CB, Chanock SJ & Dickler H (2006) Chronic granulomatous disease. Report on a national registry of 368 patients. *Medicine (Baltimore)* **79**, 155–169.

34 Test ST, Lampert M, Ossanna PJ, Thoene JG & Weiss SJ (1984) Generation of nitrogen-chlorine oxidants by human phagocytes. *J Clin Invest* **74**, 1341–1349.

35 Reeves EP, Nagl M, Godovac-Zimmermann J & Segal AW (2003) Reassessment of the microbicidal activity of reactive oxygen species and hypochlorous acid with reference to the phagocytic vacuole of the neutrophil granulocyte. *J Med Microbiol* **52**, 643–651.

36 Jahn B, Koch A, Schmidt A, Wanner G, Gehringer H, Bhakdi S & Brakhage AA (1997) Isolation and characterization of a pigmentless-conidium mutant of *Aspergillus fumigatus* with altered conidial surface and reduced virulence. *Infect Immun* **65**, 110–117.

37 Jahn B, Boukhallouk F, Lotz J, Langfelder K, Wanner G & Brakhage AA (2000) Interaction of human phagocytes with pigmentless *Aspergillus* conidia. *Infect Immun* **68**, 3736–3739.

38 Pocsi I, Miskei M, Karanyi Z, Emri T, Ayoubi P, Pusztahelyi T, Balla G & Prade RA (2005) Comparison of gene expression signatures of diamide, H_2O_2 and menadione exposed *Aspergillus nidulans* cultures – linking genome-wide transcriptional changes to cellular physiology. *BMC Genomics* **6**, 182.

39 Sheppard DC, Doedt T, Chiang LY, Kim HS, Chen D, Nierman WC & Filler SG (2005) The *Aspergillus fumigatus* StuA protein governs the up-regulation of a discrete transcriptional program during the acquisition of developmental competence. *Mol Biol Cell* **16**, 5866–5879.

40 Guzman-d, e-Pena D, Aguirre J & Ruiz-Herrera J (1998) Correlation between the regulation of sterimatocystin biosynthesis and asexual and sexual sporulation in *Emericella nidulans*. *Antonie Van Leeuwenhoek* **73**, 199–205.

41 McCluskey K (2003) The Fungal Genetics Stock Center: from molds to molecules. *Adv Appl Microbiol* **52**, 245–262.

42 Nicholson TP, Rudd BA, Dawson M, Lazarus CM, Simpson TJ & Cox RJ (2001) Design and utility of oligonucleotide gene probes for fungal polyketide synthases. *Chem Biol* **8**, 157–178.

43 Burns C, Geraghty R, Neville C, Murphy A, Kavanagh K & Doyle S (2005) Identification, cloning, and functional expression of three glutathione transferase genes from *Aspergillus fumigatus*. *Fungal Genet Biol* **42**, 319–327.

44 McCarthy E, Stack C, Donnelly SM, Doyle S, Mann VH, Brindley PJ, Stewart M, Day TA, Maule AG & Dalton JP (2004) Leucine aminopeptidase of the human blood flukes, *Schistosoma mansoni* and *Schistosoma japonicum*. *Int J Parasitol* **34**, 703–714.

45 Reeves EP, Lu H, Jacobs HL, Messina CG, Bolsover S, Gabella G, Potma OE, Warley A, Roes J & Segal A (2002) Killing activity of neutrophils is mediated through activation of proteases by K + flux. *Nature* **416**, 291–297.

46 Reiber K, Reeves EP, Neville CM, Winkler R, Gebhardt P, Kavanagh K & Doyle S (2005) The expression of selected non-ribosomal peptide synthetases in *Aspergillus fumigatus* is controlled by the availability of free iron. *FEMS Microbiol Lett* **248**, 83–91.

47 Suckau D, Resemann A, Schuerenberg M, Hufnagel P, Franzen J & Holle A (2003) A novel MALDI LIFT-TOF/TOF mass spectrometer for proteomics. *Anal Bioanal Chem* **376**, 952–965.

48 Sambrook J, Fritsch E & Maniatis T (1989) *Molecular Cloning: a Laboratory Manual*. Cold Spring Harbor Laboratory Press, Cold Spring Harbor, New York.

49 van der Lende TR, van de Kamp M, Berg M, Sjollema K, Bovenberg RA, Veenhuis M, Konings WN & Driessen AJ (2002) Delta-(1-alpha-aminoadipyl)-L-cysteinyl-D-valine synthetase, that mediates the first committed step in penicillin biosynthesis, is a cytosolic enzyme. *Fungal Genet Biol* **37**, 49–55.

50 Segal AW & Jones OT (1980) Rapid incorporation of the human neutrophil plasma membrane cytochrome b into phagocytic vacuoles. *Biochem Biophys Res Commun* **92**, 710–715.

51 Segal AW, Geisow M, Garcia R, Harper A & Miller R (1981) The respiratory burst of phagocytic cells is associated with a rise in vacuolar pH. *Nature* **290**, 406–409.

52 Cotter G, Doyle S & Kavanagh K (2000) Development of an insect model for the in vivo pathogenicity testing of yeast. *FEMS Immunol Med Micobiol* **27**, 163–169.

53 Hazen KC (1989) Participation of yeast cell surface hydrophobicity in adherence of *Candida albicans* to human epithelial cells. *Infect Immun* **57**, 1894–1900.

Supplementary material

The following supplementary material is available online:

Fig. S1. Phylogenetic analysis of adenylation (A) domains from a range of fungal nonribosomal peptide synthetases (NRPS). GenBank accession numbers for all NRPS are given in supplementary Table 1. The location of the four Aspergillus fumigatus Pes1-derived A domains is shown (*). Pes1A4 clusters with C. heterostrophus NPS4 A4 and A. brassicae NRPS1 A4, respectively. The A3 domains for all three proteins also exhibit evolutionary relatedness, but to a lesser extent.

Table S1. Genbank accession numbers of all fungal nonribosomal peptide synthetases used to construct the data in supplementary Fig. S1.

This material is available as part of the online article from http://www.blackwell-synergy.com